

# Bacterial Nanocellulose/Copper as a Robust Laccase-Mimicking Bionanozyme for Catalytic Oxidation of Phenolic Pollutants

Afomiya Animaw Achamyeleh, Biniyam Abera Ankala, Yitayal Admassu Workie, Menbere Leul Mekonnen,\* and Ebrahim M. Abda\*



Cite This: *ACS Omega* 2023, 8, 43178–43187



Read Online

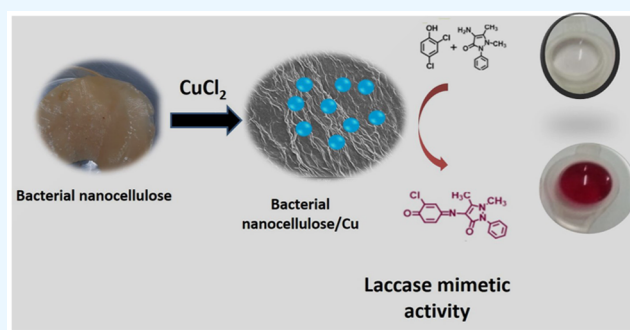
ACCESS |

Metrics & More

Article Recommendations

Supporting Information

**ABSTRACT:** Industrial effluents containing phenolic compounds are a major public health concern and thus require effective and robust remediation technologies. Although laccase-like nanozymes are generally recognized as being catalytically efficient in oxidizing phenols, their support materials often lack resilience in harsh environments. Herein, bacterial nanocellulose (BNC) was introduced as a sustainable, strong, biocompatible, and environmentally friendly biopolymer for the synthesis of a laccase-like nanozyme (BNC/Cu). A native bacterial strain that produces nanocellulose was isolated from black tea broth fermented for 1 month. The isolate that produced BNC was identified as *Bacillus* sp. strain T15, and it can metabolize hexoses, sucrose, and less expensive substrates, such as molasses. Further, BNC/Cu nanozyme was synthesized using the *in situ* reduction of copper on the BNC. Characterization of the nanozyme by scanning electron microscopy (SEM) and X-ray diffraction (XRD) confirmed the presence of the copper nanoparticles dispersed in the layered sheets of BNC. The laccase-mimetic activity was assessed using the chromogenic reaction between 2,4-dichlorophenol (2,4-DP) and 4-aminoantipyrine (4-AP) with characteristic absorption at 510 nm. Remarkably, BNC/Cu has 50.69% higher catalytic activity than the pristine Cu NPs, indicating that BNC served as an effective biomatrix to disperse Cu NPs. Also, the bionanozyme showed the highest specificity toward 2,4-DP with a  $K_m$  of 0.187 mM, which was lower than that of natural laccase. The bionanozyme retained catalytic activity across a wider temperature range with optimum activity at 85 °C, maintaining 38% laccase activity after 11 days and 46.77% activity after the fourth cycle. The BNC/Cu bionanozyme could efficiently oxidize more than 70% of 1,4-dichlorophenol and phenol in 5 h. Thereby, the BNC/Cu bionanozyme is described here as having an efficient ability to mimic laccase in the oxidation of phenolic compounds that are commonly released into the environment by industry.



## 1. INTRODUCTION

To meet the ever-increasing demands of mankind, numerous industries were established throughout the decade. These include steel, chemical, pulp and paper, and other industries that discharge significant amounts of industrial effluent containing biodegradable and nonbiodegradable substances such as polymers, heavy metals, and phenolic compounds. Given that some phenolic compounds are extremely hazardous and carcinogenic, the treatment of organic wastewater containing phenolic compounds has a significant impact on people's lives. Therefore, mechanical, chemical, and biological methods have been employed to minimize or completely eliminate phenolic compounds. The biological approach reduces, detoxifies, or mineralizes phenolic pollutants using microorganisms and their enzymes, such as laccase, and is also considered environmentally friendly.<sup>1,2</sup>

Laccases are versatile multicopper oxidases that catalyze single-electron oxidation of a diverse array of substrates, including phenolic compounds such as polyphenols, amino-

phenols, and polyamines.<sup>2,3</sup> They are widely distributed in nature and are mainly extracted from microorganisms, plants, and animals. Microbial laccase has low thermal stability, a high purification cost, and susceptibility to damage in actual industrial environments, which limits its application for environmental remediation under harsh conditions.<sup>3</sup> Enzyme mimics, as an affordable and more stable alternative, have been proposed to circumvent these restrictions.

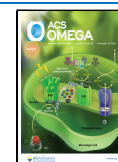
Nanozymes are nanomaterials with an intrinsic catalytic activity. Laccase-mimicking nanozymes have drawn the interest of scientists due to their effectiveness, high stability and durability, cheap cost, tunable catalytic activity, and simple

**Received:** September 8, 2023

**Revised:** October 24, 2023

**Accepted:** October 25, 2023

**Published:** November 6, 2023



manufacturing methods.<sup>4</sup> They were mainly synthesized by mixing copper ions and organic molecules, which served as scaffolds, and were used to detoxify phenolic pollutants.<sup>5–7</sup> With this framework, Shams et al. synthesized laccase-mimicking nanozyme by mixing copper ions and 1,3,5-benzene tricarboxylic acid (1,3,5-H3BTC) and reported robust catalytic activity for Amido black 10B (AB-10B) dye degradation.<sup>5</sup> Additionally, significant progress has been made in developing laccase-based nanozymes with tailored properties. By coordinating copper with biomolecules such as oligonucleotides, dipeptides, and single amino acids, researchers have developed laccase nanozymes with specific temperature and pH optima, making them suitable for various industrial applications.<sup>6–9</sup> Thereby, a laccase-mimicking nanozyme was synthesized from an organometallic framework of guanosine monophosphate (GMP) and copper to degrade hydroquinone, naphthol, catechol, and adrenaline, with catalytic performance superior to microbial laccase.<sup>6</sup> Xu et al. reported the development of a laccase-mimicking nanozyme that uses the dipeptide cysteine and aspartic acid to coordinate copper, resulting in a highly active nanozyme with optimal activity at 50 °C.<sup>7</sup>

However, the practical application of laccase nanozymes is limited by the stability of their ligands and biomolecules in harsh environments. To overcome this restriction, more work must be put into developing stable, robust laccase nanozymes that can work well in challenging environments. Biopolymers with more active sites and defined structural and functional properties are more desirable as scaffolds for copper to regulate particle formation and stabilize the resultant NPs.<sup>10</sup> Additionally, the shape, size, and stability of the NPs are influenced by the structural and functional characteristics of the biopolymer used as scaffolds.<sup>11,12</sup> Therefore, the use of biopolymers with tailored properties holds significant potential for the design of efficient nanozymes.

Bacterial nanocellulose (BNC) is a remarkable biopolymer that is produced by different types of bacteria. It is a complex macromolecule composed of  $\beta$ -D-glucopyranose. One of the most notable uses of BNC is as a catalyst carrier, thanks to its exceptional properties. It has high purity, excellent biocompatibility, and a remarkable crystallinity level of 70–80%.<sup>13,14</sup> Additionally, BNC is highly strong, both mechanically and thermally, making it a dependable choice for a wide range of applications. Microorganisms in numerous genera have the ability to produce bacterial nanocellulose, including *Gluconacetobacter*, *Aerobacter*, *Rhizobium*, *Sarcina*, *Azotobacter*, *Agrobacterium*, *Pseudomonas*, and *Alcaligenes*.<sup>15,16</sup> As a result, bacterial nanocellulose may be readily extracted from bacteria and exploited as a renewable resource to improve copper nanoparticles' ability to mimic laccase activity by providing a favorable milieu for copper.

The aim of this research was to explore the potential of BNC extracted from *Bacillus* sp. strain T15 as a scaffold for synthesizing a laccase-like nanozyme. The synthesized nanozyme was then used for the oxidation of model phenolic pollutants, which are common environmental contaminants. This research sheds valuable insights into the potential of BNC as a scaffold material for the development of advanced nanozymes with a variety of applications in environmental remediation and other fields.

## 2. EXPERIMENTAL SECTION

**2.1. Materials.** All chemicals and reagents used for this research were of analytical grade and used without further

purification. 2,4-dichlorophenol, 4-aminoantipyrine, phenol, calcium chloride ( $\text{CaCl}_2$ ), dipotassium phosphate ( $\text{K}_2\text{HPO}_4$ ), and magnesium sulfate ( $\text{MgSO}_4 \cdot 7\text{H}_2\text{O}$ ) were purchased from Alpha Chemika Andheri, West Mumbai, (India). Manganese chloride ( $\text{MnCl}_2 \cdot 4\text{H}_2\text{O}$ ), copper chloride ( $\text{CuCl}_2$ ), sodium borohydride ( $\text{NaBH}_4$ ), sodium molybdate ( $\text{Na}_2\text{MoO}_4$ ), boric acid ( $\text{H}_3\text{BO}_3$ ), acetic acid ( $\text{CH}_3\text{COOH}$ , 99%), and sodium hydroxide ( $\text{NaOH}$ ) were purchased from Unichem Chemical Reagents, Greenville County, South Carolina. TMB (3,3',5,5'-Tetramethylbenzidine) ( $\text{C}_{16}\text{H}_2\text{ON}_2$ , 99%) was obtained from Acros Organics.

**2.2. Screening and Isolation of Nanocellulose-Producing Bacteria.** The isolation of bacteria from fermented tea was done by enrichment and spread plate methods. Briefly, three bags of black tea were infused in a boiled solution of 10% (w/v) sucrose in deionized water for 5 min. The enrichment culture was fermented for 1 month at room temperature while monitoring the development of a white layer at the air–liquid interface. Cultures with a white layer at the air–liquid interface were further selected to isolate nanocellulose-producing bacteria. Then, aliquots of serially diluted samples were spread onto a Hestrin and Schramm (HS) agar medium composed of (g/L): D-glucose 20.0, peptone 5.0, yeast extract 5.0,  $\text{Na}_2\text{HPO}_4$  2.7, citric acid 1.15, and agar 15 at pH  $6.2 \pm 0.2$ .<sup>17</sup> Finally, the inoculated Petri plates were incubated at 30 °C for 5–7 days. The colonies were further streaked repeatedly until a single colony morphology was observed. Bacterial isolates were further screened for their ability to produce nanocellulose by culturing each isolate in HS broth.<sup>18</sup> Briefly, each isolate was inoculated into 10 mL of HS fermentation medium (g/L: D-glucose 20.0, peptone 5.0, yeast extract 5.0,  $\text{Na}_2\text{HPO}_4$  2.7, citric acid 1.15, and pH 6.0) in a test tube. The inoculated broths were incubated at 30 °C under static conditions for 10 days. The sample with pellicles in the air–liquid interface was an indication of BNC production.<sup>18</sup> The obtained single bacterial isolates were stored in 25% (v/v) glycerol at  $-80$  °C for future use and subsequently subcultured for refreshment when needed.

**2.3. Biosynthesis and Purification of Bacterial Nanocellulose.** After 14 days of incubation, the BNC was removed from the culture, rinsed with distilled water to remove the excess medium, and soaked in 0.1 M NaOH at 100 °C for 30 min to remove any bacteria present in the fiber. The resulting BNC was washed several times until the pH of the filtrate became neutral. Finally, the obtained BNC was dried at 60 °C in a drying oven, and the weight of the BNC was recorded.

**2.4. Characterization of Bacterial Nanocellulose.** The functional groups in the BNC produced by the potent isolate were further characterized with Fourier transform infrared (Nicolet Evolution-300) spectroscopy. Also, the morphology of the BNC was analyzed by scanning electron microscopy (FESEM JSM-6500F).

**2.5. Molecular Identification of Nanocellulose-Producing Bacteria.** Bacterial DNA extraction and PCR amplification were performed for the nanocellulose-producing bacterium, as described in ref 19. Briefly, bacterial genomic DNA was extracted using a DNA extraction kit (QIAGEN, QIAamp DNA Mini Kit) according to the manufacturer's instructions and eluted in 100  $\mu\text{L}$  of TE buffer. The eluted DNA was used as template DNA in the polymerase chain reaction (PCR) to amplify the 16S rRNA gene. The PCR mix consisted of 10  $\mu\text{L}$  of master mix (10 $\times$  Taq buffer, 10 mM

dNTPs, 25 mM MgCl<sub>2</sub>, 1 μL of Taq DNA polymerase), 1 μL of each bacterial 16S universal rRNA primer [forward primer 27-F (5-ACAGTTTGATCCTGGCTCAG-3) and reverse primer 1492-R (5-GGGTTACCTTGTACGACTT-3)], 2 μL of genomic DNA, and 6 μL of PCR-grade water. PCR amplifications were performed with a thermal cycler (model: DW-B960). For this, the standard PCR reaction conditions were maintained (initial denaturation at 94 °C for 5 min; 35 cycles consisting of template denaturation at 94 °C for 1 min, primer annealing at 55 °C for 40 s, primer extension at 72 °C for 1 min, and a final extension at 72 °C for 10 min). The PCR products were visualized by the gel documentation system after gel electrophoresis was done on a 1% agarose gel. The 16S rRNA gene was sequenced using an automated sequencer in Germany following the manufacturer's protocol (Eurofins, DE).

For phylogenetic analysis, the raw DNA sequences (DNA chromatogram) were viewed, edited using the BioEdit program, and converted into the FASTA format. Consequently, poor-quality sequence products were removed from the 3' and 5' sequence ends and assembled using MEGA X. Then, using BLASTn, the sequence data were compared to NCBI (<http://www.ncbi.nlm.nih.gov>) database and the phylogenetic analysis was performed. The phylogenetic tree was built using MEGA X with bootstrap values of 1000 replications with the maximum likelihood method<sup>20</sup> and the Kimura 2 parameter model.<sup>21</sup>

**2.6. Synthesis of Bacterial Nanocellulose-Copper (BNC/Cu) Nanozyme.** BNC/Cu nanocomposite was synthesized using the *in situ* reduction method, as described in ref 22. Briefly, 3.6 g of CuCl<sub>2</sub> was dissolved in 20 mL of deionized water and stirred for 30 min. After adjusting the pH to 8 with ammonia, the BNC was added and stirred for 30 min. Then, 1 mL of sodium borohydride was added to the mixture until a red-brown color formed. Finally, the red-brown product was rinsed off and dried in a vacuum at 60 °C overnight for further experiments.

**2.7. Characterization of Bacterial Nanocellulose-Copper (BNC/Cu) Nanozyme.** The surface morphology of the synthesized BNC/Cu nanozyme was studied by using a scanning electron microscope (FESEM JSM-6500F). The crystallinity and phase composition of the prepared nanozyme were checked by an X-ray powder diffractometer (D/MAX-2500 Bruker) with a Cu Kα source (λ = 1.5406 Å), isolated with a Ni foil filter. All absorbance measurements were conducted using a double-beam UV-vis spectrophotometer (Jasco770).

**2.8. Laccase-like Catalytic Activity of BNC/Cu Nanozyme.** The catalytic activity of BNC/Cu nanozyme was studied using 2,4-DP as substrate and 4-AP as a chromogenic agent, as described in ref 7. First, 100 μL of aqueous-dispersed BNC/Cu nanozyme was added to a mixture containing 100 μL of 4-AP (1 mg/mL) and 100 μL of 2,4-DP (1 mg/mL) in 700 μL of tris buffer (1 M, pH 6.5). The absorbance of the supernatant was then measured by using a UV-Vis spectrophotometer. Unless mentioned, this protocol was used as a standard assay for the rest of the experiments. In parallel, control experiments were performed by reacting 2,4-DP and 4-AP in the absence of nanozyme and only 2,4-DP with nanozyme.

**2.9. Steady-State Kinetic Analysis.** Kinetic studies of BNC/Cu nanozyme were performed at a fixed nanozyme concentration (1 mg/mL) by varying the concentration of 2,4-

DP (10–180 μg/L). In all of these reactions, the concentration of 4-AP was in excess at 1 mg/mL. The initial rate of reaction was then determined from the time course measurement of the absorbance at 510 nm. Then, the obtained data were fitted to the Michaelis–Menten equation (eq 2). The kinetic parameters, such as  $K_m$  and  $V_{max}$ , were then calculated using the Lineweaver–Burk plot (eq 1), which is the linear form of the Michaelis–Menten equation.

$$\frac{1}{V_0} = \frac{K_m}{V_{max}[S]} + \frac{1}{V_{max}} \quad (1)$$

$$V_0 = \frac{V_{max}}{K_m} + [S] \quad (2)$$

where  $V$  is the initial velocity,  $K_m$  is the Michaelis constant, which indicates the affinity between the enzyme and substrate,  $V_{max}$  is the maximum velocity of the reaction, and  $[S]$  is the substrate concentration.

**2.10. Effect of Reaction Parameters on the Catalytic Activity of BNC/Cu Nanozyme.** The effect of reaction parameters such as pH and mass of nanozyme on the catalytic activity of the BNC/Cu nanozyme was evaluated using a one-factor-at-a-time approach. The effect of pH on the catalytic activity of BNC/Cu nanozyme was studied by varying the solution pH from 2 to 9. Likewise, the mass of the nanozyme required for catalyzing the chromogenic reaction was optimized by conducting the reactions at various amounts of BNC/Cu (0.1–0.8 mg) at constant pH and substrate concentrations. Further, the unit activity of the nanozyme was analyzed using the initial rates measured at these masses of the nanozyme using eq 3.

$$\text{unit activity} = \left( \frac{V}{\epsilon \times l} \right) \times \left( \frac{\Delta A}{\Delta t} \right) \quad (3)$$

where  $V$  is volume,  $\epsilon$  is molar absorptivity coefficient,  $l$  is the path length,  $A$  is absorbance, and  $\Delta t$  is the change time.

**2.11. Stability and Recyclability of BNC/Cu Nanozyme.** The thermal stability of BNC/Cu was studied by conducting the standard laccase activity assay at different temperatures ranging from 25 to 100 °C in a water bath system. To study the storage stability of BNC/Cu, samples were dispersed in a buffer and stored at room temperature. Then, aliquots were taken on different days to measure their catalytic activity. The recyclability of BNC/Cu was also examined by measuring the catalytic activity at different cycles by using the standard laccase activity assay. The reaction mixture was centrifuged (at 6000 rpm for 5 min) and washed with distilled water to obtain the cleaned nanozyme, which was then used for the subsequent cycle of chromogenic reaction. The efficiency of the nanozyme in each cycle was compared by measuring the absorbance at 510 nm.

**2.12. Catalytic Oxidation of Phenolic Pollutants.** The catalytic activity of the BNC/Cu nanozyme for the oxidation of different phenolic substrates was tested by subjecting each phenolic compound to a catalytic oxidation reaction in the presence of 4-AP. Briefly, 100 μL of each phenolic compound (1 mg/mL) was dissolved in tris buffer (1 M, pH 6.8, 700 μL) and mixed with 100 μL of 4-AP (1 mg/mL) and BNC/Cu nanozyme (1 mg/mL, 100 μL). While the reaction was allowed to proceed, the absorbance of the resulting solution was measured at various time intervals. Accordingly, the percentage of the oxidized substrate was calculated using eq 4. The

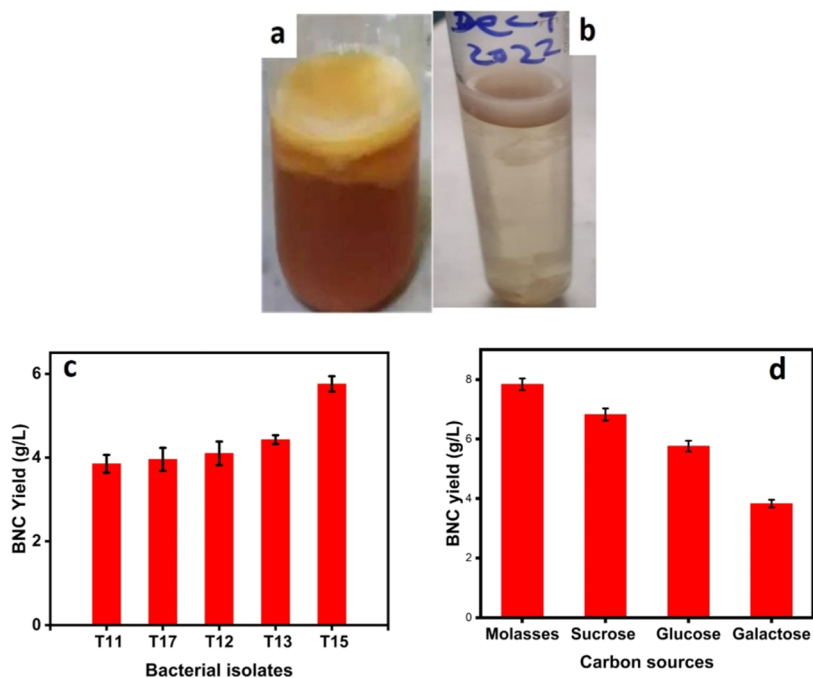


**Figure 1.** Isolation and screening of nanocellulose-producing bacteria from an enriched culture. (a) Formation of white pellicles at the air–liquid interface; (b) growth of bacterial isolate in HS medium; (c) BNC yield by the bacterial isolates in HS media; and (d) BNC production by bacterial isolate T15 from different carbon sources.

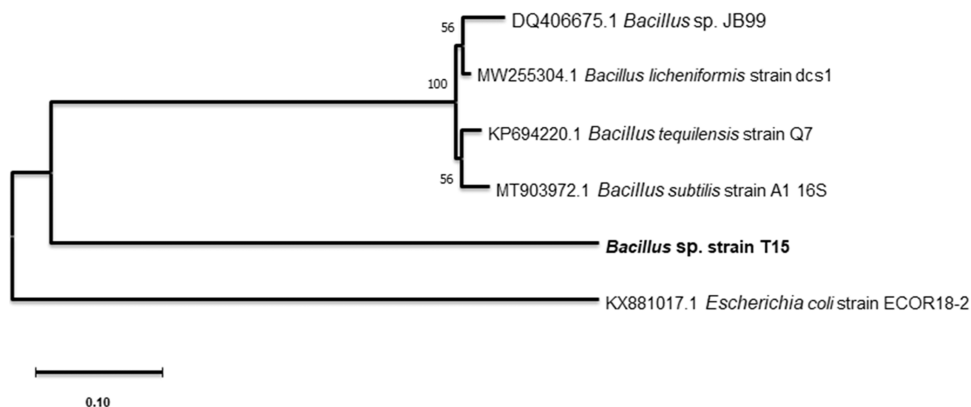


**Figure 2.** Phylogenetic analysis of partial 16S rRNA gene of *Bacillus* isolate (bolded and coded with “T15”) forming cluster with *Bacillus* species.

concentrations at different times were calculated from the absorbance using Beer’s Law.

$$\% \text{oxidation} = \frac{C_t}{C_0} \times 100 \quad (4)$$

where  $C_0$  is the initial concentration and  $C_t$  is the concentration at time  $t$ .

### 3. RESULTS AND DISCUSSION

**3.1. Isolation and Screening of Nanocellulose-Producing Bacteria.** Forty-six pure bacterial isolates were recovered from an enriched tea culture that formed white pellicles at the air–liquid interface (Figure 1a). To further study each isolate for nanocellulose production, 17 isolates were selected based on their cultural characteristics (Figure S1). Thereby, 29.4% of the isolates formed white pellicles at the air–liquid interface after being cultured in HS broth for 14 days (Figure 1b). The most evident bacterial nanocellulose production was exhibited by the bacterial isolates designated as

T11, T12, T13, T15, and T17 (Figure 1c). Further, bacterial nanocellulose production by the five isolates varied as well; T15 produced the highest amount ( $5.76 \pm 0.18$  g/L), followed by T13 ( $4.42 \pm 0.10$  g/L), and T11 produced the least ( $3.85 \pm 0.21$ ) (Figure 1c). As a result, isolate T15 produced BNC that was comparable to that of *Gluconacetobacter xylinus* ZHCJ618<sup>23</sup> and *Komagataeibacter rhaeticus* strain P 1463.<sup>23</sup>

As the carbon source is considered to be a factor limiting the production and application of BNC, isolate T15 was further evaluated for its ability to produce BNC from different carbon sources such as galactose, sucrose, and molasses. Consequently, BNC production of isolate T15 was  $7.84 \pm 0.19$ ,  $6.83 \pm 0.20$ , and  $3.83 \pm 0.12$  g/L in molasses, sucrose, and galactose media, respectively (Figure 1d). When molasses was used as the carbon source instead of glucose, the BNC yield of T15 was 36% higher (Figure 1d). Molasses is considered an inexpensive and readily available substrate for bacterial strains to produce nanocellulose.

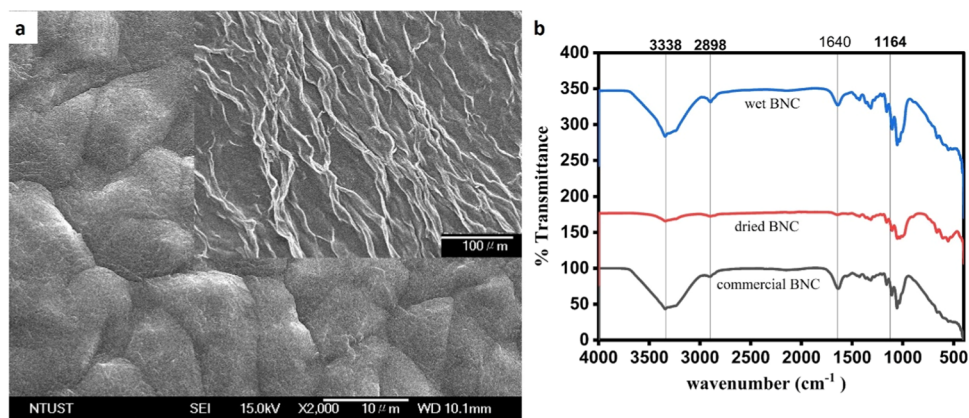


Figure 3. (a) SEM image of BNC recovered from isolate T15; (b) FTIR spectra of BNC.

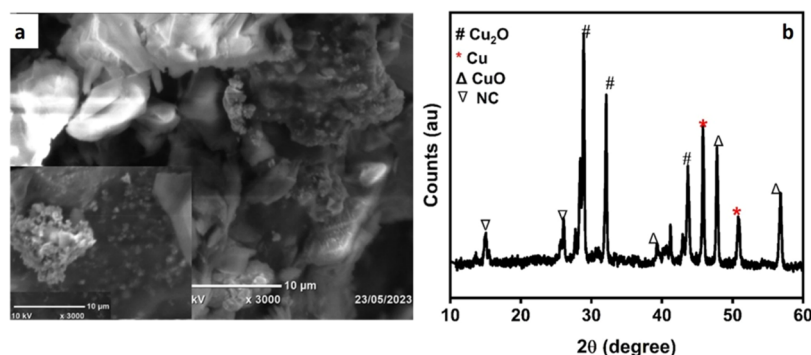


Figure 4. (a) SEM image and (b) XRD pattern of BNC/Cu nanozyme.

**3.2. Molecular Identification of Nanocellulose-Producing Bacterium.** The macroscopic and microscopic characteristics of the T15 isolate were examined using selected biochemical assay and gram staining. Accordingly, T15 was Gram-positive rod-shaped bacteria with a rough margin (Table S1). Further, it was identified by PCR amplification of a region that carries most of the diversity information. As a result, 16S rRNA gene sequence analysis revealed that T15 belongs to the genus *Bacillus*, showing 100% similarity to several species of *Bacillus*. Thus, partial 16S rRNA gene sequences from members of *Bacillus* sp. were used to construct the phylogenetic tree by including additional isolates from the NCBI database (Figure 2). The bacterial isolate T15 formed a cluster with *Bacillus* species and was named *Bacillus* sp. strain T15. However, many BNC producers are Gram-negative and belong to the genus *Komagataeibacter*, including *Komagataeibacter sacrofermentans* H110 and *Komagataeibacter hansenii* C110.<sup>24</sup> Recently, many Gram-positive bacteria with the ability to produce bacterial nanocellulose have been isolated from different sources, including *Lactiplantibacillus plantarum*<sup>25</sup> and *Bacillus licheniformis* ZBT2.<sup>26</sup> In particular, a thermophilic strain of *B. licheniformis* ZBT2 secreted exopolysaccharides to form pellicles at the air–liquid interface. Therefore, the *Bacillus* sp. strain T15 isolated in this study could indicate that the ability to produce BNC is widespread in the genus *Bacillus*.

**3.3. Characterization of Bacterial Nanocellulose Produced by T15.** Initially, the functional groups of extracted BNC from the bacterial isolate T15 were compared to those of commercial bacterial nanocellulose (Cellobio Company). As shown in Figure 3b, the FTIR spectral analysis confirmed the similarity between the functional groups of the BNC and the

reference molecule (commercial cellulose). As seen in Figure 3b, the FTIR spectrum of T15 BNC showed broad absorption peaks at 3334 and 3338  $\text{cm}^{-1}$ , which correspond to the OH stretching of dried and wet BNC, respectively. This indicates the presence of a hydroxyl group, which forms bonds with different molecules such as metal nanoparticles and polymers, and so on.<sup>27</sup> The weak bands at 2898.962 and 2902  $\text{cm}^{-1}$  for the wet and dry BNC, respectively, represent C–H stretching of the aliphatic group. The peak at 1641  $\text{cm}^{-1}$  in the wet BNC representing the O–H bending vibration diminished when the BNC was dried. This could be due to loss of moisture during the drying process.<sup>12</sup> Further, the band at 1164  $\text{cm}^{-1}$  showed the C–O–C bond of the antisymmetric bridge stretching of  $\beta$ -1,4-glycosidic bonds, indicating that the monomeric glucose units of BNC are connected by glycosidic bonds.<sup>27</sup> Taken together, the FITR analyses indicated the characteristics of vibrational bands expected from the bacterial nanocellulose structure and were consistent with commercial BNC used as a control. Further, the morphology of the bacterial nanocellulose was observed by scanning electron microscopy. Figure 3a shows the SEM image of BNC from isolate T15 in HS media and dried in an oven at 50 °C. As observed in the micrographs, the BNC appeared as thick-layered sheets, typically consistent with bacterial isolates producing BNC in a similar type of culture media.<sup>28,29</sup>

**3.4. Synthesis and Characterization of BNC/Cu Nanozyme.** The BNC/Cu nanozyme was synthesized by the *in situ* reduction of copper on the BNC and further characterized by SEM/EDX and XRD. The morphology of the prepared BNC/Cu nanozyme was examined using SEM. As shown in Figure 4a, the bacterial nanocellulose appeared as

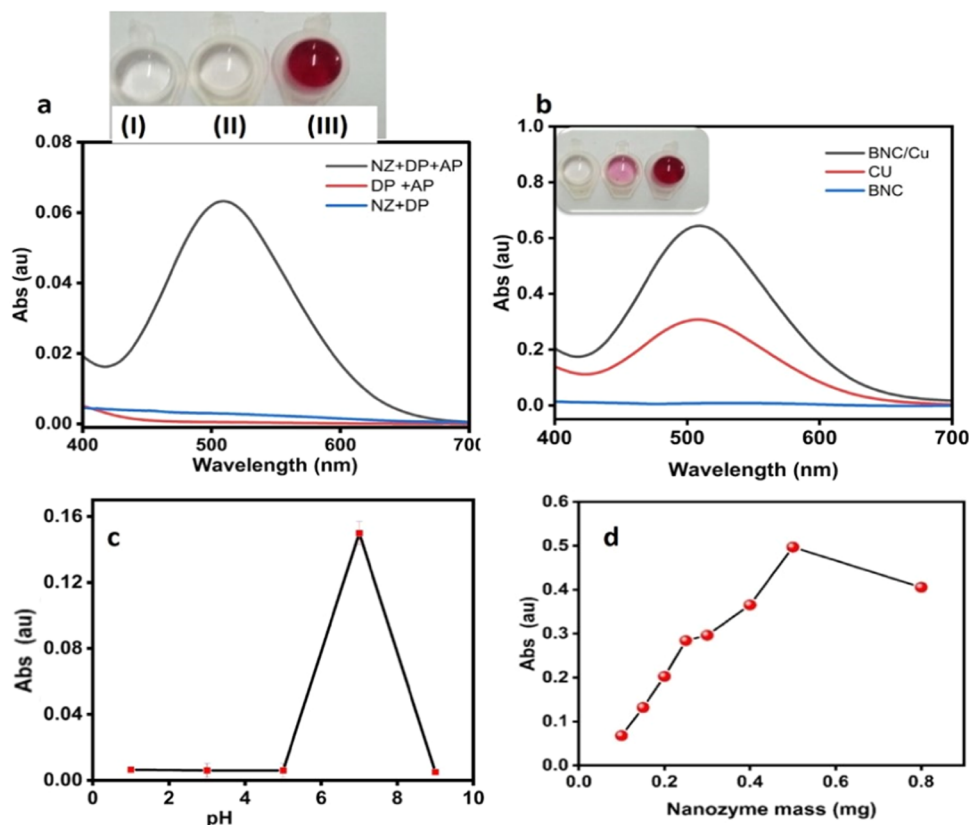


**Figure 5.** (a) Preliminary laccase activity test ((I) DP + AP; (II) BNC/Cu + DP; (III) BNC/Cu + DP + AP); (b) comparison of the laccase activity of BNC/Cu, Cu NPs and BNC; effect of (c) pH; and (d) nanozyme mass on the laccase activity BNC/Cu.

layered sheets on which the copper nanoparticles were dispersed. Further, the EDX spectrum confirmed the presence of Cu, C, and O, which are the expected elemental compositions of the nanocomposite (Figure S2). The lower composition of copper (0.74%) is consistent with the laccase enzyme structure, in which the catalytic centers are in lower proportions.<sup>30</sup>

The phase composition and crystallinity of the prepared nanozyme were studied using powdered XRD. The XRD pattern (Figure 4b) of BNC/Cu shows two peaks at  $15.1^\circ$  and  $25.9^\circ$ , which correspond to the diffraction from (100) and (110) planes of  $1\alpha$  and  $1\beta$  crystalline bacterial nanocellulose, respectively.<sup>31</sup> The peaks at  $2\theta$   $45.8^\circ$  and  $50.7^\circ$  correspond to diffraction from (111) and (200) planes of copper nanoparticles, while the peaks at  $2\theta$   $28.9^\circ$ ,  $32.1^\circ$ , and  $43.6^\circ$  are characteristics of diffraction from (110), (111), and (200) planes of cubic  $\text{Cu}_2\text{O}$ . In addition, the peaks at  $2\theta$   $39.26^\circ$ ,  $47.8^\circ$ , and  $56.9^\circ$  represent diffraction from (111),  $(-202)$ , and (202) planes of  $\text{CuO}$ , respectively (JCPDS #01-080-0076). The results show the prepared nanozyme constitutes three phases of copper, which is consistent with the oxidation states of copper found in natural laccase. The average crystallite sizes of copper nanoparticles and BNC calculated by the Sheerer equation were found to be 33.22 and 28.03 nm, respectively.

### 3.5. Laccase-Mimicking Catalytic Activity of BNC/Cu.

The laccase mimicking ability of the BNC/Cu nanozyme was studied using 2,4-DP as a model substrate and 4-AP as a chromogenic agent in a buffer (pH 7). As shown in Figure 5a, the oxidized product of 2,4-DP reacted with 4-AP in the presence of the nanozyme to generate a red adduct with a characteristic absorption peak at 510 nm. Meanwhile, reactions

containing the phenolic substrate without the nanozyme and only 2,4-DP with the nanozyme remained colorless, indicating the role of BNC/Cu as a mimetic laccase nanozyme (Figure 5a). Furthermore, as shown in Figure 5b, BNC/Cu has a 50.69% higher catalytic activity than the pristine copper nanoparticles, pointing out the role of the bacterial nanocellulose as a scaffold for the distribution of the copper nanoparticles, which would otherwise tend to aggregate and subsequently lose activity.<sup>32</sup> Hence, the addition of BNC enhanced the laccase-mimetic activity of copper nanoparticles by preventing aggregation.

To further optimize the catalytic conditions, the pH, nanozyme mass, and composite mass were investigated. The pH stability of enzymes is vital for the environmental remediation of recalcitrant pollutants. Consequently, the catalytic assay was carried out at various pH values ranging from 2 to 9. Figure 5c shows that the catalytic activity of the BNC/Cu nanozyme was low in acidic and basic media and peaked at near-neutral pH. The nanozyme works best in a wider pH range, often between 5 and 8, which is consistent with previous reports.<sup>7</sup> Furthermore, the effect of the precursor ratio was optimized by varying the mass of  $\text{CuCl}_2$  and BNC. As shown in Figure S3, a BNC/Cu ratio of 2:1.5 resulted in optimal activity. As the copper mass increased above 1.5, the laccase-mimetic activity decreased, possibly due to the aggregation of Cu NPs at this BNC concentration. Similarly, the effect of nanozyme amount on laccase-mimetic activity was studied at various BNC/Cu concentrations at a fixed substrate concentration (100  $\mu\text{L}$ , 1 mg/L). The activity of the nanozyme increased with increasing mass, as shown in Figure 5d, peaking

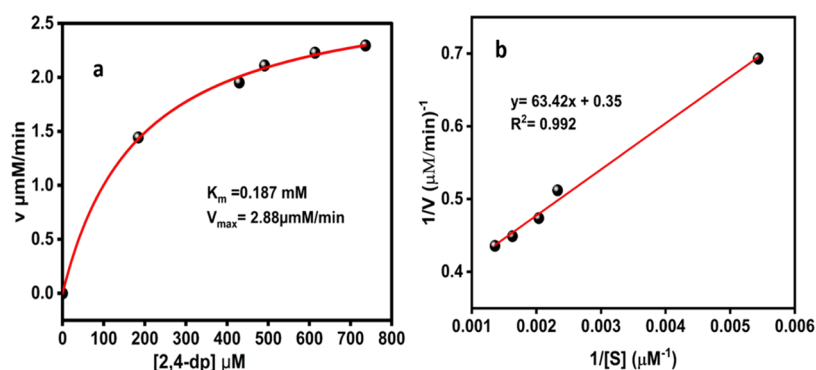


**Figure 6.** (a) Micheal–Menten plot; (b) Lineweaver–Burk plots of the nanozyme catalyzed reaction at different 2,4-DP concentrations.

at 0.5 mg of BNC/Cu and then decreasing as the mass continued to increase.

**3.6. Steady-State Kinetics of BNC/Cu Nanozyme.** The steady-state kinetics for the catalytic oxidation reaction were studied by varying the concentration of 2,4-DP at a fixed BNC/Cu nanozyme concentration. As can be seen in Figure 6a, the rate of the chromogenic reaction followed a typical Michaelis–Menten model. The kinetic parameters  $K_m$  and  $V_{max}$  calculated from the Lineweaver–Burk plot were 0.187 mM and 2.881  $\mu\text{M}/\text{min}$ , respectively (Figure 6b). A summary of the kinetic parameters for recently published natural laccase and other nanozymes is presented in Table 1. The BNC/Cu

**Table 1.** Survey of Kinetic Parameters for the Recently Reported Natural Laccase and Laccase-Mimicking Nanozymes

catalyst	substrate	$K_m$ (mM)	$V_{max}$ ( $\text{M min}^{-1}$ )	reference
Cu/GMP	2,4-DP	0.59	$1.3 \times 10^{-5}$	6
CH/Cu	2,4-DP	0.42	$1.22 \times 10^{-4}$	7
$\text{Cu}_2\text{O}_3$	2,4-DP	0.203	$10^{-7}$	34
I–Cu	2,4-DP	0.17	$4.1 \times 10^{-7}$	35
natural laccase	2,4-DP	0.65	$5.78 \times 10^{-5}$	6
BNC/Cu	2,4-DP	0.18	$4.8 \times 10^{-8}$	this work

nanozyme subsequently exhibited equivalent, if not greater, catalytic activity for the oxidation of phenolic chemicals. The  $K_m$  value of the BNC/Cu nanozyme, which is used to assess the affinity of nanozymes for substrates, was lower than that of a natural laccase enzyme,<sup>33</sup> indicating a stronger affinity for 2,4-DP.

**3.7. Catalytic Stability and Recyclability of BNC/Cu.** Nanozymes are helpful in several applications, including wastewater treatment and soil bioremediation, due to their stability and recyclability. Natural laccases frequently lose their catalytic activity upon exposure to high temperatures and extended storage. With this framework, the thermal stability of the BNC/Cu nanozyme was investigated by incubating the enzymes at different temperatures ranging from 25 to 100 °C. As shown in Figure 7a, BNC/Cu nanozyme activity increased with increasing temperature, reaching its optimum at 85 °C. However, above 85 °C, the laccase mimic ability decreased by 35.4 and 50% at 90 and 100 °C, respectively. Overall, the BNC/Cu nanozyme had excellent catalytic ability over a wide temperature range compared with natural laccase enzymes. For instance, an entirely novel laccase enzyme produced by cyanobacteria has a maximum activity at 30 °C and retains 10% of its activity at 80 °C.<sup>36</sup> Additionally, the prepared

nanozyme showed enhanced thermal activity compared to a cysteine-aspartic-copper nanozyme, which showed maximum activity at 50 °C.<sup>7</sup> Further, to examine the temporal stability, the BNC/Cu nanozyme was dispersed in a buffer, and its activity was measured at different times. As seen in Figure 7b, the BNC/Cu nanozyme retained 38% laccase activity after 11 days. Hence, the thermal and temporal stability results suggest the robustness of the prepared nanozyme for environmental remediation.

Recyclability is another essential requirement for the practical application of enzymes and often limits the use of natural enzymes in wastewater treatment plants because they often lose their activity in hostile environments.<sup>37</sup> Therefore, the recyclability of BNC/Cu was evaluated by performing a laccase activity test with the recovered nanozyme after each test cycle. Thereby, the BNC/Cu nanozyme maintained 46.77% of its activity after the fourth cycle (Figure 7c). These results showed better recyclability than immobilized laccase used for pharmaceutical waste degradation, with a recyclability of 38.31%.<sup>38</sup> The decrease in activity after the four cycles could be due to leaching out of copper nanoparticles from the nanocellulose matrix, which reduces the copper units in the nanozyme.<sup>6,34</sup>

**3.8. Oxidation of Phenolic Compounds.** Due to their widespread industrial applications, phenolic compounds are often discharged with wastewater from paint, textile, and other industries and persist in the environment. Hence, from the viewpoint of environmental safety and public health, finding a simple yet effective remediation tool for phenolic compounds is critical. The ability of the BNC/Cu laccase nanozyme to degrade phenolic compounds was investigated by using two model phenolic compounds: phenol and 2,4-dichlorophenol. The oxidation efficiencies at different time intervals were calculated using eq 4. The concentration of the oxidized product was calculated from the absorbance at 510 nm by using Beer’s law. As seen in Figure 8, the nanozyme converted almost 50% of both substrates in 3 h, whereas more than 70% of the substrates were converted in 5 h. The results indicated a comparable performance of the nanozyme, which reported more than 90 and 70% conversion in 10 h, respectively.<sup>7</sup>

## 4. CONCLUSIONS

In summary, the BNC/Cu bionanozyme was demonstrated to be an effective laccase mimic for the catalytic oxidation of phenolic compounds. Using the BNC from *Bacillus* sp. strain T15 as an effective biomatrix for dispersing Cu NPs, the synthesized BNC/Cu bionanozyme demonstrated 50.69% higher catalytic activity than virgin Cu NPs. This demonstrates

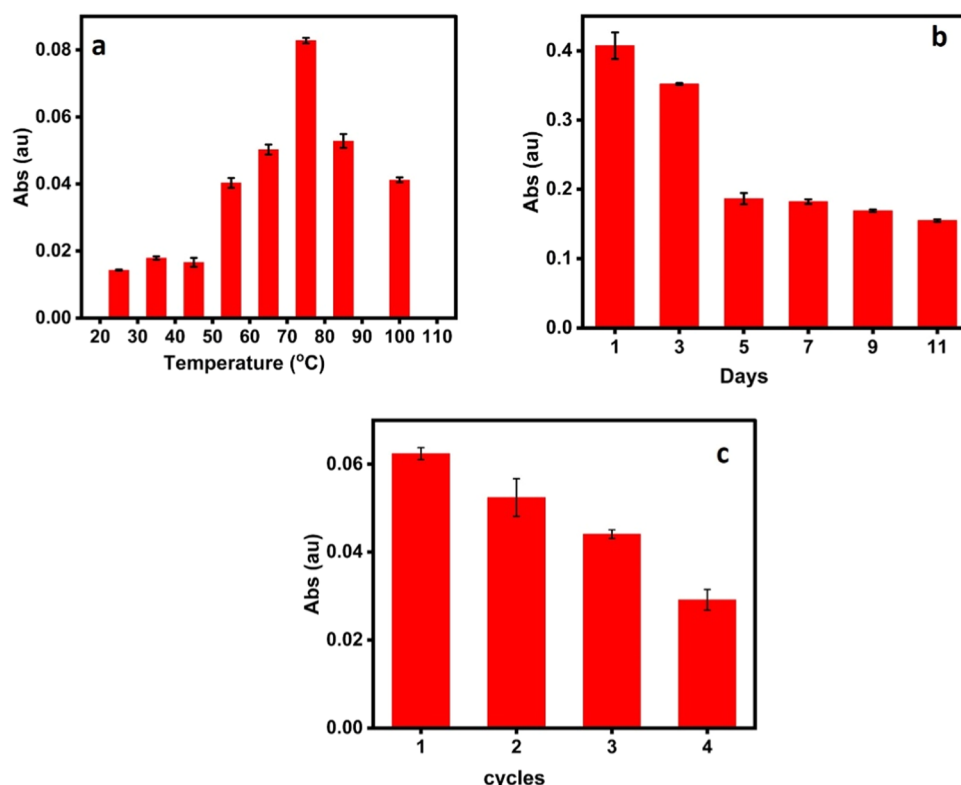


Figure 7. (a) Thermal stability; (b) temporal stability; (c) recyclability of BNC/Cu.

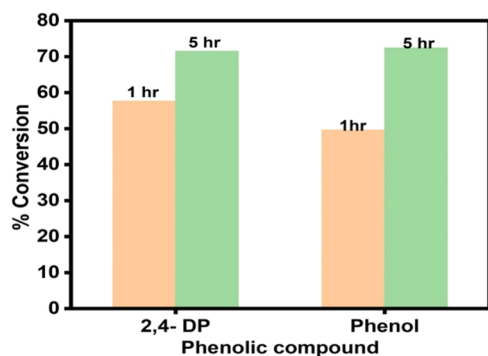


Figure 8. Catalytic oxidation efficiency of the BNC/Cu nanozyme for different phenolic compounds at different times.

that the use of BNC improves electron transport during catalytic processes, which increases the mimetic laccase activity of copper nanoparticles. The bionanozyme showed robust thermal and temporal stability as well as pH-dependent catalytic activity for the oxidation of phenolic compounds. Further, the bionanozyme showed the highest specificity toward 2,4-DP with a  $K_m$  of 0.187 mM, which is lower than natural laccase. The bionanozyme efficiently oxidizes more than 70% of 1,4-dichlorophenol and phenol in 5 h. Finally, the use of low-cost substrates for BNC production is particularly attractive for reducing production costs, thereby increasing its applications. In this sense, BNC productivity by *Bacillus* sp. strain T15 was improved by 36% when molasses was used as a carbon substrate. Therefore, this strain can be used for BNC production to synthesize a highly effective bionanozyme with potential applications in environmental remediation.

## ■ ASSOCIATED CONTENT

### Data Availability Statement

The data that support the findings of this study are available on request from the corresponding authors. However, the partial 16S rRNA sequence of *Bacillus* sp. strain T15 has been deposited in the National Center for Biotechnology Information (<https://www.ncbi.nlm.nih.gov/>) under the accession numbers OR713745.

### Supporting Information

The Supporting Information is available free of charge at <https://pubs.acs.org/doi/10.1021/acsomega.3c06847>.

Growth of bacterial isolates recovered from enriched culture on HS, EDX spectrum of BNC/Cu, the effect of precursor's ratio on the nanozyme activity, and cultural and morphological characteristics of nanocellulose-producing bacterial isolate T15 (PDF)

## ■ AUTHOR INFORMATION

### Corresponding Authors

**Member Leul Mekonnen** – Industrial Chemistry Department, Addis Ababa Science and Technology University, Addis Ababa P.O. Box 1647, Ethiopia; Nanotechnology Center of Excellence, Addis Ababa Science and Technology University, Addis Ababa P.O. Box 1647, Ethiopia; [orcid.org/0000-0001-9617-853X](https://orcid.org/0000-0001-9617-853X); Email: [member.leul@aastu.edu.et](mailto:member.leul@aastu.edu.et)

**Ebrahim M. Abda** – Biotechnology Department and Biotechnology and Bio-processing Center of Excellence, Addis Ababa Science and Technology University, Addis Ababa P.O. Box 1647, Ethiopia; [orcid.org/0000-0002-2475-9703](https://orcid.org/0000-0002-2475-9703); Email: [ebrexmama@gmail.com](mailto:ebrexmama@gmail.com), [ebrahim.mama@aastu.edu.et](mailto:ebrahim.mama@aastu.edu.et)



## Authors

**Afomiya Animaw Achamyeleh** – Biotechnology Department, Addis Ababa Science and Technology University, Addis Ababa P.O. Box 1647, Ethiopia

**Biniyam Abera Ankala** – Industrial Chemistry Department, Addis Ababa Science and Technology University, Addis Ababa P.O. Box 1647, Ethiopia

**Yitayal Admassu Workie** – Industrial Chemistry Department, Addis Ababa Science and Technology University, Addis Ababa P.O. Box 1647, Ethiopia; Nanotechnology Center of Excellence, Addis Ababa Science and Technology University, Addis Ababa P.O. Box 1647, Ethiopia

Complete contact information is available at:

<https://pubs.acs.org/10.1021/acsomega.3c06847>

## Notes

The authors declare no competing financial interest.

## ACKNOWLEDGMENTS

The authors are grateful to Addis Ababa Science and Technology University for the financial support under the University's Interdisciplinary Internal Research Grant Number IG 07/2022.

## REFERENCES

- (1) Arora, P. K.; Bae, H. Bacterial Degradation of Chlorophenols and Their Derivatives. *Microb. Cell Fact.* **2014**, *13* (1), 31.
- (2) Rostami, A.; Abdelrasoul, A.; Shokri, Z.; Shirvandi, Z. Applications and Mechanisms of Free and Immobilized Laccase in Detoxification of Phenolic Compounds — A Review. *Korean J. Chem. Eng.* **2022**, *39* (4), 821–832.
- (3) Arregui, L.; Ayala, M.; Gómez-Gil, X.; Gutiérrez-Soto, G.; Hernández-Luna, C. E.; Herrera de los Santos, M.; Levin, L.; Rojo-Domínguez, A.; Romero-Martínez, D.; Saparrat, M. C. N.; Trujillo-Roldán, M. A.; Valdez-Cruz, N. A. Laccases: Structure, Function, and Potential Application in Water Bioremediation. *Microb. Cell Fact.* **2019**, *18* (1), No. 200.
- (4) Ma, H.; Zheng, N.; Chen, Y.; Jiang, L. Laccase-like Catalytic Activity of Cu-Tannic Acid Nanohybrids and Their Application for Epinephrine Detection. *Colloids Surf., A* **2021**, *613*, No. 126105.
- (5) Shams, S.; Ahmad, W.; Memon, A. H.; Wei, Y.; Yuan, Q.; Liang, H. Facile Synthesis of Laccase Mimic Cu/H3BTC MOF for Efficient Dye Degradation and Detection of Phenolic Pollutants. *RSC Adv.* **2019**, *9* (70), 40845–40854.
- (6) Liang, H.; Lin, F.; Zhang, Z.; Liu, B.; Jiang, S.; Yuan, Q.; Liu, J. Multicopper Laccase Mimicking Nanozymes with Nucleotides as Ligands. *ACS Appl. Mater. Interfaces* **2017**, *9* (2), 1352–1360.
- (7) Xu, X.; Wang, J.; Huang, R.; Qi, W.; Su, R.; He, Z. Preparation of Laccase Mimicking Nanozymes and Their Catalytic Oxidation of Phenolic Pollutants. *Catal. Sci. Technol.* **2021**, *11* (10), 3402–3410.
- (8) Makam, P.; Yamijala, S. S. R. K. C.; Bhadram, V. S.; Shimon, L. J. W.; Wong, B. M.; Gazit, E. Single Amino Acid Bionanozyme for Environmental Remediation. *Nat. Commun.* **2022**, *13* (1), No. 1505.
- (9) Tian, S.; Zhang, C.; Yu, M.; Li, Y.; Fan, L.; Li, X. Buffer Species-Dependent Catalytic Activity of Cu-Adenine as a Laccase Mimic for Constructing Sensor Array to Identify Multiple Phenols. *Anal. Chim. Acta* **2022**, *1204*, No. 339725.
- (10) Cai, Y.; Zhou, J.; Huang, J.; Zhou, W.; Wan, Y.; Cohen Stuart, M. A.; Wang, J. Rational Design of Polymeric Nanozymes with Robust Catalytic Performance via Copper-Ligand Coordination. *J. Colloid Interface Sci.* **2023**, *645*, 458–465.
- (11) Xu, Y.; Zhou, Z.; Deng, N.; Fu, K.; Zhu, C.; Hong, Q.; Shen, Y.; Liu, S.; Zhang, Y. Molecular Insights of Nanozymes from Design to Catalytic Mechanism. *Sci. China Chem.* **2023**, *66* (5), 1318–1335.
- (12) Hendrikse, H. C.; Aguirre, A.; van der Weijden, A.; Meeussen, A. S.; Neira D'Angelo, F.; Noorduyn, W. L. Rational Design of

Bioinspired Nanocomposites with Tunable Catalytic Activity. *Cryst. Growth Des.* **2021**, *21* (8), 4299–4304.

(13) Klemm, D.; Cranston, E. D.; Fischer, D.; Gama, M.; Kedzior, S. A.; Kralisch, D.; Kramer, F.; Kondo, T.; Lindström, T.; Nietzsche, S.; Petzold-Welcke, K.; Rauchfuß, F. Nanocellulose as a Natural Source for Groundbreaking Applications in Materials Science: Today's State. *Mater. Today* **2018**, *21* (7), 720–748.

(14) Zhong, C. Industrial-Scale Production and Applications of Bacterial Cellulose. *Front. Bioeng. Biotechnol.* **2020**, *8*, No. 605374, DOI: 10.3389/fbioe.2020.605374.

(15) Zhong, C.; Zhang, G.-C.; Liu, M.; Zheng, X.-T.; Han, P.-P.; Jia, S.-R. Metabolic Flux Analysis of *Gluconacetobacter Xylinus* for Bacterial Cellulose Production. *Appl. Microbiol. Biotechnol.* **2013**, *97* (14), 6189–6199.

(16) Gao, M.; Li, J.; Bao, Z.; Hu, M.; Nian, R.; Feng, D.; An, D.; Li, X.; Xian, M.; Zhang, H. A Natural in Situ Fabrication Method of Functional Bacterial Cellulose Using a Microorganism. *Nat. Commun.* **2019**, *10* (1), No. 437.

(17) Hestrin, S.; Schramm, M. Synthesis of Cellulose by *Acetobacter Xylinum*. II. Preparation of Freeze-Dried Cells Capable of Polymerizing Glucose to Cellulose. *Biochem. J.* **1954**, *58* (2), 345–352.

(18) Lahiri, D.; Nag, M.; Dutta, B.; Dey, A.; Sarkar, T.; Pati, S.; Edinur, H. A.; Abdul Kari, Z.; Mohd Noor, N. H.; Ray, R. Bacterial Cellulose: Production, Characterization, and Application as Antimicrobial Agent. *Int. J. Mol. Sci.* **2021**, *22* (23), No. 12984, DOI: 10.3390/ijms222312984.

(19) Abda, E. M.; Adugna, Z.; Assefa, A. Elevated Level of Imipenem-Resistant Gram-Negative Bacteria Isolated from Patients Attending Health Centers in North Gondar, Ethiopia. *Infect. Drug Resist.* **2020**, *13*, 4509–4517.

(20) Kumar, S.; Stecher, G.; Li, M.; Knyaz, C.; Tamura, K. MEGA X: Molecular Evolutionary Genetics Analysis across Computing Platforms. *Mol. Biol. Evol.* **2018**, *35*, 1547.

(21) Kimura, M. A Simple Method for Estimating Evolutionary Rates of Base Substitutions through Comparative Studies of Nucleotide Sequences. *J. Mol. Evol.* **1980**, *16* (2), 111–120.

(22) Musa, A.; Ahmad, M. B.; Hussein, M. Z.; Mohd Izham, S.; Shameli, K.; Abubakar Sani, H. Synthesis of Nanocrystalline Cellulose Stabilized Copper Nanoparticles. *J. Nanomater.* **2016**, *2016*, No. 2490906.

(23) Zhang, W.; Wang, X.; Qi, X.; Ren, L.; Qiang, T. Isolation and Identification of a Bacterial Cellulose Synthesizing Strain from Kombucha in Different Conditions: *Gluconacetobacter Xylinus* ZHCJ618. *Food Sci. Biotechnol.* **2018**, *27* (3), 705–713.

(24) Revin, V. V.; Liyas'kina, E. V.; Sapunova, N. B.; Bogatyreva, A. O. Isolation and Characterization of the Strains Producing Bacterial Cellulose. *Microbiology* **2020**, *89* (1), 86–95.

(25) Saleh, A. K.; El-Gendi, H.; Soliman, N. A.; El-Zawawy, W. K.; Abdel-Fattah, Y. R. Bioprocess Development for Bacterial Cellulose Biosynthesis by Novel *Lactiplantibacillus Plantarum* Isolate along with Characterization and Antimicrobial Assessment of Fabricated Membrane. *Sci. Rep.* **2022**, *12* (1), No. 2181.

(26) Bagewadi, Z. K.; Bhavikatti, J. S.; Muddapur, U. M.; Yaraguppi, D. A.; Mulla, S. I. Statistical Optimization and Characterization of Bacterial Cellulose Produced by Isolated Thermophilic *Bacillus Licheniformis* Strain ZBT2. *Carbohydr. Res.* **2020**, *491*, No. 107979.

(27) Beluhan, S.; Herceg, F.; Leboš Pavunc, A.; Djaković, S. Preparation and Structural Properties of Bacterial Nanocellulose Obtained from Beetroot Peel Medium. *Energies* **2022**, *15* (24), No. 9374, DOI: 10.3390/en15249374.

(28) Costa, A. F. S.; Almeida, F. C. G.; Vinhas, G. M.; Sarubbo, L. A. Production of Bacterial Cellulose by *Gluconacetobacter Hansenii* Using Corn Steep Liquor As Nutrient Sources. *Front. Microbiol.* **2017**, *8*, No. 2027, DOI: 10.3389/fmicb.2017.02027.

(29) Santos, S. M.; Carbajo, J. M.; Quintana, E.; Ibarra, D.; Gomez, N.; Ladero, M.; Eugenio, M. E.; Villar, J. C. Characterization of Purified Bacterial Cellulose Focused on Its Use on Paper Restoration. *Carbohydr. Polym.* **2015**, *116*, 173–181.

(30) Lei, Y.; He, B.; Huang, S.; Chen, X.; Sun, J. Facile Fabrication of 1-Methylimidazole/Cu Nanozyme with Enhanced Laccase Activity for Fast Degradation and Sensitive Detection of Phenol Compounds. *Molecules* **2022**, *27* (15), No. 4712, DOI: 10.3390/molecules27154712.

(31) Potivara, K.; Phisalaphong, M. Development and Characterization of Bacterial Cellulose Reinforced with Natural Rubber. *Materials* **2019**, *12*, 2323.

(32) Conway, J. R.; Adeleye, A. S.; Gardea-Torresdey, J.; Keller, A. A. Aggregation, Dissolution, and Transformation of Copper Nanoparticles in Natural Waters. *Environ. Sci. Technol.* **2015**, *49* (5), 2749–2756.

(33) Wang, X.; Liu, J.; Qu, R.; Wang, Z.; Huang, Q. The Laccase-like Reactivity of Manganese Oxide Nanomaterials for Pollutant Conversion: Rate Analysis and Cyclic Voltammetry. *Sci. Rep.* **2017**, *7* (1), No. 7756.

(34) Maity, T.; Jain, S.; Solra, M.; Barman, S.; Rana, S. Robust and Reusable Laccase Mimetic Copper Oxide Nanozyme for Phenolic Oxidation and Biosensing. *ACS Sustainable Chem. Eng.* **2022**, *10* (4), 1398–1407.

(35) Wang, J.; Huang, R.; Qi, W.; Su, R.; He, Z. Construction of Biomimetic Nanozyme with High Laccase- and Catecholase-like Activity for Oxidation and Detection of Phenolic Compounds. *J. Hazard. Mater.* **2022**, *429*, No. 128404.

(36) Afreen, S.; Shamsi, T. N.; Baig, M. A.; Ahmad, N.; Fatima, S.; Qureshi, M. I.; Hassan, M. I.; Fatma, T. A Novel Multicopper Oxidase (Laccase) from Cyanobacteria: Purification, Characterization with Potential in the Decolorization of Anthraquinonic Dye. *PLoS One* **2017**, *12* (4), No. e0175144.

(37) Adamian, Y.; Lonappan, L.; Alokpa, K.; Agathos, S. N.; Cabana, H. Recent Developments in the Immobilization of Laccase on Carbonaceous Supports for Environmental Applications - A Critical Review. *Front. Bioeng. Biotechnol.* **2021**, *9*, No. 778239, DOI: 10.3389/fbioe.2021.778239.

(38) Masjouidi, M.; Golgoli, M.; Ghobadi Nejad, Z.; Sadeghzadeh, S.; Borghei, S. M. Pharmaceuticals Removal by Immobilized Laccase on Polyvinylidene Fluoride Nanocomposite with Multi-Walled Carbon Nanotubes. *Chemosphere* **2021**, *263*, No. 128043.